# Resource Allocation for Outdoor Visible Light Communications with Energy Harvesting Capabilities

Amr M. Abdelhady, Osama Amin, Anas Chaaban, and Mohamed-Slim Alouini
Computer, Electrical and Mathematical Sciences and Engineering (CEMSE) Division,
King Abdullah University of Science and Technology (KAUST),
Thuwal, Makkah Province, Saudi Arabia.
E-mail: {amr.abdelhady, osama.amin, anas.chaaban, slim.alouini}@kaust.edu.sa

***Abstract*—Visible light communication (VLC) is a promising technology that can support high data rate services for outdoor mass gathering night events while permitting energy harvesting. In this paper, a VLC system is considered where a transmitter sends data to multiple users with energy harvesting capabilities. This multi-user VLC scenario can be supported using time division multiple access (TDMA). The achievable rates using TDMA are expressed in terms of the allocated resources per user, represented by average optical intensity and time slots. This allocation is to be optimized in order to maximize the average spectral efficiency while meeting power and quality-of-service (QoS) constraints. Herein, QoS is defined as a worst-case guaranteed rate and a minimum harvested energy. To solve this optimization, the optimality conditions are first derived. Then, an efficient algorithm is developed based on the derived conditions, and its near-optimality is verified through several numerical evaluations. The obtained performance is also compared to lower-complexity algorithms, thus reflecting the performance-complexity trade-off of these algorithms.**

## I. Introduction

Recently, optical wireless communications (OWC) received a lot of research attention to mitigate the spectrum scarcity problem in wireless communications. OWC offers a high speed solution that can meet the exponential increase of wireless communication demand. It can be implemented in different forms such as free space optical (FSO) communications and visible light communications (VLC). FSO offers a high speed solution for different applications such as backhaul links. On the other hand, it may suffer from some impairments such as pointing errors, scattering, turbulence and terminal swing. VLC offers high speed data communication thanks to large modulation bandwidth of the light emitting diodes (LEDs) used recently for illumination [1].

VLC has several advantages over radio frequency (RF) communications, which encourages considering it for next generation wireless networks. For instance, VLC uses the wide visible light spectrum that extends from a wavelength of 380 nm to 750 nm. Additionally, VLC can benefit from existing infrastructure which makes it cheaper than setting up new RF networks. Furthermore, VLC offers a ubiquitous indoor and outdoor service where illumination is required. Dependency on line-of-sight is one of the main challenges that prevents delivering the required service. In such cases, hybrid RF and VLC systems should be used to complement each other. Another serious challenge is the interference coming from ambient lights such as sunlight and other indoor light sources. Most research on VLC focused on indoor applications [2], [3].

Outdoor VLC has not received much attention except for vehicular applications [4], [5]. In this paper, we shed light on one of the promising outdoor VLC applications, namely, serving mass gathering night events. A high degree of illumination is required to support such events, e.g., social or sports events. Using VLC in such circumstances should be encouraged for many reasons. First, the absence of sunlight interference, which allows achieving a good performance. Additionally, the high illumination intensity requirement implies the availability of strong signal that is capable of serving a suitable number of users at high data rates. Moreover, using VLC in such scenarios reduces costs as there is no need to set up a new wireless network or use movable base stations, thereby reducing interference and sparing the RF spectrum. Furthermore, it makes (optical) energy harvesting more promising and viable thanks to the high illumination intensity requirement.

Motivated by this, we consider an outdoor VLC system with a powerful light source used to illuminate an area that accommodates a large number of users. The light source is also used for information transmission using VLC, and the users have the capability to harvest light energy. We study the problem of allocating the VLC system resources based on time division multiple access (TDMA) to provide a downlink service with a quality-of-service (QoS) requirement. We assume that energy harvesting must fulfill a specific portion of the circuits energy consumption. We derive the optimality conditions for this allocation, and based thereon, we develop an iterative algorithm that allocates the average optical intensity and association time for each user. Then, we compare its performance with two simplified algorithms having different complexities in order to elaborate the spectral efficiency (SE) performance - complexity trade-off. Finally, we present extensive simulations that confirm our algorithm's capabilities compared with the optimal solution and show the average SE with respect to different system parameters.

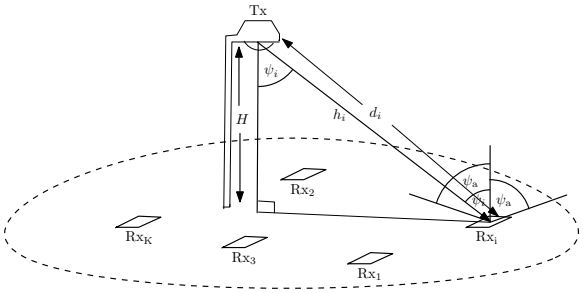


Fig. 1. System Model

## II. System Model

Consider an outdoor VLC system consisting of a powerful transmitter serving $K$ users using dynamic TDMA with modulation bandwidth of $B_{\rm v}$ Hz, where users have visible light energy harvesting capabilities and they are assumed to harvest energy all the time. The received signal by the $i$-th user can be modeled as

$$y_i = h_i s_i + n_i, \tag{1}$$

where $s_i \geq 0$ is the current used to transmit a symbol to the $i$-th user, $h_i$ represents the VLC channel gain between the transmitter and the $i$-th receiver, and $n_i$ is a zero mean additive white Gaussian noise with variance $\sigma_n^2$. The electrical to optical conversion efficiency is assumed to be one, and hence $s_i$ can also be interpreted as optical intensity.

The transmission frame interval duration $T$ seconds is divided between users such that user $i$ is allotted $\tau_i T$ seconds during each transmission frame, where $\sum_{i=1}^{K} \tau_i = 1$. Due to practical limitations, it is required that $\tau_i \geq \tau_{\min}\ \forall i$. The average energy consumption at the transmitter per transmitted frame must satisfy $T\sum_{i=1}^{K} \tau_i \mathbb{E}\{s_i^2\} = E_{\rm v}$, where $E_{\rm v}$ is the VLC transmitter energy consumption per transmission frame. In this work, we adopt the quasi-static channel model presented in [6] where the channel gain $h_i$ between the transmitter and receiver $i$ depends solely on the relative position of the receiver with respect to the transmitter, and is given by:

$$h_i = \frac{(m+1)A_{\rm PD}R_{\rm PD}}{2\pi d_i^2}\cos^{m+1}(\psi_i)\text{rect}\left(\frac{\psi_i}{\psi_{\rm a}}\right), \tag{2}$$

where $m = \ln 2/\ln(\cos(\phi_{\rm a}))$ is the Lambertian order, $\phi_{\rm a}$ is the semi-angle at half-power of the light source emission pattern, $A_{\rm PD}$ is the effective photo-detector area, $d_i$ is the distance between the transmitter and user $i$, $\psi_i$ is the angle between the incident light ray and the normal to the photo-detector plane, $\psi_{\rm a}$ is the field of view of the user's receiver, and rect$(x)$ is the rectangular function defined as rect$(x) = 1$ if $|x| \leq 1$, and 0 otherwise. We assume perfect knowledge of $h_i\ \forall i$ at the transmitter.

The system QoS requirements are represented as a worst-case user rate requirement and an energy harvesting requirement per user. The former is given by $R_{{\rm wc},i} \geq R_{\rm th}$ for some $R_{\rm th}$, where $R_{{\rm wc},i}$ is defined as the rate that can be guaranteed for user $i$ when given a fraction $\tau_{\min}$ of time, and located at the same distance from the transmitter as the worst user. The latter is given by $E_{{\rm h},i} \geq \beta P_{\rm cr}\tau_i T$, where $E_{{\rm h},i}$ is the amount of harvested energy by user $i$, which can't be stored and must be used instantaneously to cover a portion $\beta$ of its circuitry energy consumption $P_{\rm cr}\tau_i T$ with $P_{\rm cr}$ being the power used by receiver circuitry (node $i$ is active for a fraction $\tau_i$ of time). Next, we discuss the SE maximization problem.

## III. Spectral Efficiency Optimization

In this section, we study the resource allocation problem of the downlink of a VLC system to maximize its global SE. We express the overall system SE using the achievable rate for VLC systems presented in [7] with $s_i \sim$ Exponential$(1/x_i)$ as

$$\eta_{\rm SE}(\mathbf{x}, \boldsymbol{\tau}) = \frac{1}{2}\sum_{i=1}^{K} \tau_i \log_2\left(1+\gamma_i x_i^2\right), \tag{3}$$

where $\mathbf{x} = (x_1, x_2, \ldots, x_K)$ is the average current allocation vector, $\boldsymbol{\tau} = (\tau_1, \tau_2, \ldots, \tau_K)$ is the time fraction allocation vector, $\gamma_i$ is the $i$-th user channel-to-noise ratio defined as $\gamma_i = \frac{e}{2\pi}h_i^2/\sigma_n^2$, and $x_i = \mathbb{E}\{s_i\}$. The system average transmission power is $P_{\rm M} \triangleq \frac{E_{\rm v}}{T}$ Watts, i.e., $\sum_{i=1}^{K}\tau_i x_i^2 = P_{\rm M}$ (since $\mathbb{E}\{s_i^2\} = x_i^2$). In order to account for the receiver energy harvesting requirements, we define $E_{{\rm h},i}$ as $E_{\rm h,i} = 0.75\frac{\rm V_T}{I_o}h_i^2 T\sum_{j=1}^{K}\tau_j x_j^2$, where $\rm V_T$ is the thermal voltage (mVolt) and $I_o$ is the dark saturation current of the photo-detector.[1] Finally, according to the used achievable rate expression and the definition of $R_{{\rm wc},i}$, we can write $R_{{\rm wc},i} = \frac{B_{\rm v}\tau_{\min}}{2}\log_2\left(1+\gamma_{\min}x_i^2\right)$, where $\gamma_{\min} = \min_i \gamma_i$. Thus, we formulate the optimization problem as follows:

$$\begin{aligned}
\textbf{(P1)}\quad \max_{\mathbf{x},\boldsymbol{\tau}}\quad & \eta_{\rm SE}(\mathbf{x},\boldsymbol{\tau}) \\
\text{subject to}\quad & \text{C1}: \sum_i \tau_i x_i^2 = P_{\rm M},\ \text{C2}: \sum_i \tau_i = 1 \\
& \text{C3}: 0.75\frac{\rm V_T}{I_o}h_i^2\sum_j \tau_j x_j^2 \geq \beta P_{\rm cr}\tau_i \quad \forall i \\
& \text{C4}: \tau_i \geq \tau_{\min} \quad \forall i,\ \text{C5}: R_{{\rm wc},i} \geq R_{\rm th}\ \forall i.
\end{aligned}$$

Note that C3 is equivalent to $\tau_i \leq \tau_{{\max},i}\ \forall i$, where $\tau_{{\max},i} = 0.75\frac{\rm V_T}{I_o}h_i^2\frac{P_{\rm M}}{\beta P_{\rm cr}}$, as $\sum_{j=1}^{K}\tau_j x_j^2 = P_{\rm M}$. Moreover, C5 can be mapped to a minimum average current allocation constraint: $x_i \geq x_{\min} \triangleq \sqrt{\frac{1}{\gamma_{\min}}\left(2^{\frac{2R_{\rm th}}{B_{\rm v}\tau_{\min}}}-1\right)},\ \forall i$. It can be noticed that $\textbf{(P1)}$ is not a convex optimization problem due to non-concavity of its objective function in terms of the optimization parameters, and since the set defined by C1 and C2 is not a convex set. Therefore, we use the transformation of variables $z_i = \tau_i x_i^2$, to reformulate $\textbf{(P1)}$ as follows:

$$\begin{aligned}
\textbf{(}\tilde{\textbf{P1}}\textbf{)}\quad \max_{\mathbf{z},\boldsymbol{\tau}}\quad & \tilde{\eta}_{\rm SE}(\mathbf{z},\boldsymbol{\tau}) = \sum_{i=1}^{K}\tau_i \ln\left(1+\frac{\gamma_i z_i}{\tau_i}\right) \\
\text{subject to}\quad & \text{C1}: \sum_{i=1}^{K} z_i = P_{\rm M},\ \text{C2}: \sum_{i=1}^{K}\tau_i = 1 \\
& \text{C3}: \tau_i \leq \tau_{{\max},i} \quad \forall i,\ \text{C4}: \tau_i \geq \tau_{\min}, z_i \geq z_{\min}\ \forall i,
\end{aligned}$$

[1] Here, for mathematical tractability, we use the upper bound on harvested energy from VLC cell given in [8].

TABLE I
INEQUALITY CONSTRAINTS MULTIPLIERS CONFIGURATIONS. HERE, $\tau_i^*$ AND $z_i^*$ DENOTE THE OPTIMAL $\tau_i$ AND $z_i$, RESPECTIVELY.

| | | $o_i = 0$ | $o_i \neq 0$ |
|---|---|---|---|
| $\nu_i = 0$ | $\kappa_i = 0$ | **Case 1:** $\frac{z_i^*}{\tau_i^*} = \frac{1}{\mu} - \frac{1}{\gamma_i}$ and $\ln\left[\frac{\gamma_i}{\mu}\right] - 1 + \frac{\mu}{\gamma_i} = \lambda$ | **Case 4:** $\frac{z_{\min}}{\tau_i^*} = \frac{1}{\mu - o_i} - \frac{1}{\gamma_i}$ and $\ln\left[\frac{\gamma_i}{\mu - o_i}\right] + \frac{\mu - \gamma_i - o_i}{\gamma_i} = \lambda$ |
| | $\kappa_i \neq 0$ | **Case 3:** $\frac{z_i^*}{\tau_{\min}} = \frac{1}{\mu} - \frac{1}{\gamma_i}$ and $\ln\left[\frac{\gamma_i}{\mu}\right] - 1 + \frac{\mu}{\gamma_i} + \kappa_i = \lambda$ | **Case 5:** $\frac{z_{\min}}{\tau_i^*} = \frac{1}{\mu - o_i} - \frac{1}{\gamma_i}$ and $\ln\left[\frac{\gamma_i}{\mu - o_i}\right] + \frac{\mu - \gamma_i - o_i}{\gamma_i} + \kappa_i = \lambda$ |
| $\nu_i \neq 0$ | $\kappa_i = 0$ | **Case 2:** $\frac{z_i^*}{\tau_{\min}} = \frac{1}{\mu} - \frac{1}{\gamma_i}$ and $\ln\left[\frac{\gamma_i}{\mu}\right] - 1 + \frac{\mu}{\gamma_i} - \nu_i = \lambda$ | **Case 6:** $\frac{z_{\min}}{\tau_i^*} = \frac{1}{\mu - o_i} - \frac{1}{\gamma_i}$ and $\ln\left[\frac{\gamma_i}{\mu - o_i}\right] + \frac{\mu - \gamma_i - o_i}{\gamma_i} - \nu_i = \lambda$ |

where $\mathbf{z} = (z_1, z_2, \ldots, z_K)$ is the power allocation vector, and $z_{\min} = \tau_{\min} x_{\min}^2$. The objective function of $(\tilde{\mathbf{P1}})$ is a concave function in both $\mathbf{z}, \boldsymbol{\tau}$, because it is the perspective transform of $\ln(1 + \gamma_i z_i)$ which is a concave function in $\mathbf{z}$ [9]. Further, all the constraints are affine. Therefore, $(\tilde{\mathbf{P1}})$ is a convex optimization problem. and the Karush-Kuhn-Tucker (KKT) conditions guarantee global optimality.

The Lagrangian formulation of $(\tilde{\mathbf{P1}})$ is given by:

$$\begin{aligned}\mathcal{L} = &\sum_{i=1}^{K} \tau_i \ln\left(1 + \frac{\gamma_i z_i}{\tau_i}\right) + \mu\left(P_{\mathrm{M}} - \sum_i z_i\right) \\ &+ \sum_{i=1}^{K} o_i (z_i - z_{\min}) + \sum_{i=1}^{K} \nu_i (\tau_{\max,i} - \tau_i) \\ &+ \lambda\left(1 - \sum_{i=1}^{K} \tau_i\right) + \sum_{i=1}^{K} \kappa_i (\tau_i - \tau_{\min}) \end{aligned} \tag{4}$$

The KKT conditions of $(\tilde{\mathbf{P1}})$ can be summarized as:

$$\frac{\partial \mathcal{L}}{\partial z_i} = \frac{\gamma_i}{1 + \gamma_i z_i / \tau_i} - \mu + o_i = 0 \tag{5}$$

$$\frac{\partial \mathcal{L}}{\partial \tau_i} = \ln\left(1 + \frac{\gamma_i z_i}{\tau_i}\right) - \frac{\gamma_i z_i}{\tau_i + \gamma_i z_i} - \nu_i - \lambda + \kappa_i = 0 \tag{6}$$

$$o_i \geq 0, \quad \nu_i \geq 0, \quad \kappa_i \geq 0 \tag{7}$$

$$\begin{aligned}&\tau_i \geq \tau_{\min}, \quad z_i \geq z_{\min}, \quad \tau_i \leq \tau_{\max,i} \\ &0 = o_i (z_i - z_{\min}) = \nu_i (\tau_i - \tau_{\max,i}) = \kappa_i (\tau_i - \tau_{\min})\end{aligned} \tag{8}$$

$\forall i$, and $\sum_{i=1}^{K} z_i = P_{\mathrm{M}}$, $\sum_{i=1}^{K} \tau_i = 1$. The convexity of $(\tilde{\mathbf{P1}})$ implies that strict complementary slackness applies [9], such that $o_i = 0$ if and only if (iff) $z_i > z_{\min}$ and $o_i > 0$ iff $z_i = z_{\min}$ $\forall i$. Similarly, $\kappa_i = 0$ iff $\tau_i > \tau_{\min}$, $\kappa_i > 0$ iff $\tau_i = \tau_{\min}$, $\nu_i = 0$ iff $\tau_i < \tau_{\max,i}$, and $\nu_i > 0$ iff $\tau_i = \tau_{\max,i}$, $\forall i$.

We assume without loss of generality that $\gamma_1 \geq \gamma_2 \geq \cdots \geq \gamma_K$, then it follows that $\tau_{\max,1} \geq \tau_{\max,2} \geq \cdots \geq \tau_{\max,K}$. For any $i$, we have many possibilities in terms of the active constraints for the Lagrange multipliers associated with inequalities $(\nu_i, o_i, \kappa_i)$, resulting in numerous KKT stationarity conditions as shown in Table I. It can be noticed that only one user at most can satisfy the stationarity conditions represented by Case 1 in Table I, since the contrary leads to a contradiction.

To solve the KKT system of equations analytically without limiting the solutions to any structure, complexity will be exponential in terms of $K$ since we will need to try different combinations of Cases 1–6 for each user. In order to reduce the complexity, inspired by the positive monotonicity of the objective function in $\boldsymbol{\tau}$ (cf. Appendix),

**Algorithm I**

**Input** $I, P_{\mathrm{M}}, z_{\min}, \tau_{\min}, \beta, \gamma_i, \tau_{\max,i} \quad \forall i \in \{1, \ldots, K\}$
**Initialize** $\eta_{\mathrm{SE}}^{\max} = 0$, $j = l = K$, $n = 1$, where $n \equiv |\boldsymbol{\tau'}|$
**while** $n \leq K$
  **if** $n > 1$
    **Execute** Algorithm I-a
  **else**
    **Execute** Algorithm I-b
  **end if**
  $n \leftarrow n + 1$
**end while**

we limit our space of solutions to ones having the following structure: $\mathbf{z}^* = \left[z_1^*, \ldots, z_j^*, z_{\min}, \ldots, z_{\min}\right]$, $\boldsymbol{\tau}^* = \left[\tau_{\max,1}, \ldots, \tau_{\max,f-1}, \tau_f^*, \ldots, \tau_l^*, \tau_{\min}, \ldots, \tau_{\min}\right]$.

Using this solution structure, along with the fact that no more than one user can fall into Case 1 in Table I, two possibilities can occur based on $|\boldsymbol{\tau'}|$, the cardinality of the set $\boldsymbol{\tau'} = \{i : \tau_{\min} < \tau_i < \tau_{\max,i}\}$, namely, (a) $|\boldsymbol{\tau'}| > 1$ and (b) $|\boldsymbol{\tau'}| = 1$. A different procedure is applied for each possibility, as illustrated in Algorithm I. Those procedures, denoted Algorithms I-a and I-b are described next.

**(a) If $|\boldsymbol{\tau'}| > 1$:** Then, the solution structure would impose $j \geq f$, since the contrary makes more than one user fall into Case 1 in Table I, leading to a contradiction in the KKT conditions. Here two cases should be considered: (i) $j = f$ and (ii) $j > f$.

**(a.i) For $j = f$:** We set

$$z_i^* = f_i(\mu) \triangleq \tau_{\max,i}\left(\frac{1}{\mu} - \frac{1}{\gamma_i}\right), \ \forall i \in U_2 \tag{9}$$

$$\tau_i^* = z_{\min}\gamma_i \left(\frac{1}{r_i} - 1\right)^{-1}, \ \forall i \in U_4, \tag{10}$$

where $r_i = \frac{\mu - o_i}{\gamma_i}$ and $U_x$ represents the set of user indices belonging to Case $x$, i.e., $U_2 \triangleq \{1, \ldots, j-1\}$ and $U_4 \triangleq \{j+1 \ldots l\}$. By rewriting the second equation presented under Case 4 in Table I in terms of $r_i$, we get $-\ln(r_i) - 1 + r_i - \lambda = 0$, $\forall i \in U_4$, which can be solved for $r_i$ to get $r_i = -\mathcal{W}_0\left(-e^{-(\lambda+1)}\right)$ (the proof is omitted for lack of space), where $\mathcal{W}_0(.)$ is the Lambert function [10]. Then,

$$\tau_i^* = g_i(\lambda), \ \forall i \in U_4 \tag{11}$$

$$\tau_j^* = 1 - \sum_{i \in U_3} g_i(\lambda) - \sum_{i=1}^{f-1} \tau_{\max,i} - (K - l)\tau_{\min} \tag{12}$$

where $g_i(\lambda) \triangleq z_{\min}\gamma_i \left( \frac{1}{-\mathcal{W}_0\left(-e^{-(\lambda+1)}\right)} - 1 \right)^{-1}$, and

$$z_j^* = \tau_j^* \left( \frac{1}{\mu} - \frac{1}{\gamma_j} \right) \tag{13}$$

where $\mu$ is obtained by solving

$$\ln\left(\frac{\gamma_j}{\mu}\right) - 1 + \frac{\mu}{\gamma_j} = \lambda \Rightarrow \frac{\mu}{\gamma_j} = -\mathcal{W}_0\left(-e^{-(\lambda+1)}\right). \tag{14}$$

By substituting (11)–(14) in $\sum_{i=1}^{K} z_i = P_{\mathrm{M}}$, we get all the unknown primal variables in terms of $\lambda$ and reduce the system of equations to the following equation:

$$\left(1 - \sum_{i=1}^{f-1} \tau_{\max,i} - (K-l)\,\tau_{\min} - \sum_{i\in U_3} g_i(\lambda)\right) \times \left(\frac{1}{-\gamma_j \mathcal{W}_0\left(-e^{-(\lambda+1)}\right)} - \frac{1}{\gamma_j}\right) + \sum_{i\in U_2} f_i\left(-\gamma_j \mathcal{W}_0\left(-e^{-(\lambda+1)}\right)\right) = P_{\mathrm{M}} - (K-j)\,z_{\min} \tag{15}$$

It can be proved that the left-hand side of (15) is monotonically increasing in $\lambda$, and hence it admits a unique solution which can be found using the bisection method. By backward substitution, we can get all the unknown primal variables, and then the dual variables can be calculated. This is illustrated in lines 8–19 in Algorithm I-a.

**(a.ii) For $j > f$:** We have $z_i^* = f_i(\mu)$, $\forall i \le j$. So, we solve $\sum_{i=1}^{K} z_i = P_{\mathrm{M}}$ for $\mu$. Then, we get all the unknown $\mathbf{z}$ variables by backward substitution. Similarly, $\tau_i^* = g_i(\lambda)$. We solve $\sum_{i=1}^{K} \tau_i = 1$ for $\lambda$. Afterwards, all unknown $\boldsymbol{\tau}$ variables are obtained. We then calculate the rest of dual variables. This is illustrated in lines 21–30 in Algorithm I-a.

**(b) If $|\boldsymbol{\tau'}| = 1$:** Then, $f = l$ with $\tau_l^* = 1 - \sum_{i=1}^{f-1} \tau_{\max,i} - \tau_{\min}\,(K-l)$, and $z_i^* = \tau_i^* \left(\frac{1}{\mu} - \frac{1}{\gamma_i}\right)$, $\forall i \ge j$, where $\mu$ can be obtained by solving $\sum_{i=1}^{K} z_i = P_{\mathrm{M}}$. With this in mind, we search for $j \in \{1,\ldots,K\}$ and $l \in \{1,\ldots,K\}$ that satisfy the KKT conditions. This is illustrated in Algorithm I-b.

In summary, Algorithm I proceeds through three composite stages. The first stage scans values of $|\boldsymbol{\tau'}|$ where it is assumed to be one initially, but it is incremented by one after each failed iteration (KKT conditions were not satisfied). In the second stage, we look over all possible sets $\boldsymbol{\tau'}$ with equal cardinality, for one which yields a feasible time allocation (lines 1–5 in Algorithms I-a and I-b). For every feasible set $\boldsymbol{\tau'}$, the third stage loops over the possible configurations for $\boldsymbol{z}$ variables ($j$ values), where the primal and dual variables are calculated, the solutions are checked for feasibility and compared to the best feasible solution found so far $\eta_{\mathrm{SE}}^{\max}$ (lines 6 onwards in Algorithms I-a and I-b). If the current solution has a better objective function value than $\eta_{\mathrm{SE}}^{\max}$, we save the current solution and update $\eta_{\mathrm{SE}}^{\max}$, then the KKT conditions are checked to indicate whether the current calculated solution is optimal or not.

**Algorithm I-a**

1: **for** $l = K : -1 : n$
2: $t \leftarrow \sum_{i=1}^{l-n} \tau_{\max,i} + (K-l)\,\tau_{\min}$
3: **if** $t < 1$ and $(K-l)\,\tau_{\min} < 1 - t < \sum_{i=l-n+1}^{l} \tau_{\max,i}$
4: $\tau_i \leftarrow \tau_{\max,i}$, $\forall i \le l-1$ and $\tau_i \leftarrow \tau_{\min}$, $\forall i \ge l+1$
5: $j \leftarrow l - n + 1$
6: **while** $j \ge 1$
7: $z_i \leftarrow z_{\min}$, $\forall i > j$
8: **if** $j = l - n + 1$
9: **Solve** (14) for $\mu$ and (15) for $\lambda$
10: **Get** $\tau_j$ and $z_j$ from (12) and (13), respectively
11: **Compute** $z_i$ from (9) $\forall i \in U_2$
12: **Compute** $\tau_i$ from (11) $\forall i \in U_3$
13: **if** $\mathbf{z}$ and $\boldsymbol{\tau}$ are feasible, and $\tilde{\eta}_{\mathrm{SE}}(\mathbf{z}, \boldsymbol{\tau}) \ge \eta_{\mathrm{SE}}^{\max}$
14: $\mathbf{z}^* \leftarrow \mathbf{z}$, $\boldsymbol{\tau}^* \leftarrow \boldsymbol{\tau}$, $\eta_{\mathrm{SE}}^{\max} \leftarrow \tilde{\eta}_{\mathrm{SE}}(\mathbf{z}, \boldsymbol{\tau})$
15: **end if**
16: **Compute** $o_i$, $\kappa_i$, and $\nu_i$ using (5) and (6) $\forall i$
17: **if** KKT conditions are satisfied
18: $\mathbf{z}^* \leftarrow \mathbf{z}$, $\boldsymbol{\tau}^* \leftarrow \boldsymbol{\tau}$, **Terminate.**
19: **end if**
20: **else**
21: **Solve** (12) for $\lambda$ with $\tau_j = 0$.
22: **Compute** $\tau_i$ from (11) $\forall i \in U_3$
23: **Solve** (14) for $\mu$ with $\tau_j = 0$.
24: **Compute** $z_i$ from (9) $\forall i \in U_2$
25: **if** $\mathbf{z}$ and $\boldsymbol{\tau}$ are feasible and $\tilde{\eta}_{\mathrm{SE}}(\mathbf{z}, \boldsymbol{\tau}) \ge \eta_{\mathrm{SE}}^{\max}$
26: $\mathbf{z}^* \leftarrow \mathbf{z}$, $\boldsymbol{\tau}^* \leftarrow \boldsymbol{\tau}$, $\eta_{\mathrm{SE}}^{\max} \leftarrow \tilde{\eta}_{\mathrm{SE}}(\mathbf{z}, \boldsymbol{\tau})$
27: **end if**
28: **Compute** $o_i$, $\kappa_i$, and $\nu_i$ using (5) and (6) $\forall i$
29: **if** KKT conditions are satisfied
30: $\mathbf{z}^* \leftarrow \mathbf{z}$, $\boldsymbol{\tau}^* \leftarrow \boldsymbol{\tau}$, **Terminate.**
31: **end if**
32: **end if**
33: $j \leftarrow j - 1$
34: **end while**
35: **end if**
36: **end for**

## IV. Lower complexity algorithms

**Algorithm II:** Algorithm I consists of three composite iterative stages where the worst case complexity of each is $O(K)$, resulting in an overall complexity of $O\left(K^3\right)$. In order to reduce the complexity, we can modify line 3 of Algorithm I, to have $n \le 1$ instead of $n \le K$. This forces the solution to have $|\boldsymbol{\tau'}| = 1$, and guarantees finding a feasible solution at a complexity of $O\left(K^2\right)$, since this reduces the first stage of Algorithm I to one iteration.

**Algorithm III:** By delving more towards the low-complexity extreme of the performance-complexity trade-off, we can find a solution with lower complexity by allocating the resources as shown in Algorithm III. In this algorithm, the time budget is poured such that all users at first are allocated the minimum amount of time $\tau_{\min}$, then the remaining budget

**Algorithm I-b**

**for** $l = K : -1 : 1$
  $t \leftarrow \sum_{i=1}^{l-1} \tau_{\max,i} + (K-l)\,\tau_{\min}$
  **if** $t < 1$ and $\tau_{\min} < 1 - t < \tau_{\max,l}$
    $\tau_l \leftarrow 1 - t$ and $\tau_i \leftarrow \tau_{\max,i}$, $\forall i \leq l-1$
    $\tau_i \leftarrow \tau_{\min}$, $\forall i \geq l+1$, $j \leftarrow K$
    **while** $j \geq 1$
      $z_i \leftarrow z_{\min}$, $\forall i > j$
      $\mu \leftarrow \sum_{i=1}^{K} \tau_i / \left(P_{\mathrm{M}} + \sum_{i=1}^{K} \tau_i/\gamma_i\right)$
      $z_i \leftarrow \tau_i \left(1/\mu - 1/\gamma_i\right) \quad \forall i \leq j$
      **if** $\mathbf{z}$ and $\boldsymbol{\tau}$ are feasible and $\tilde{\eta}_{\mathrm{SE}}(\mathbf{z}, \boldsymbol{\tau}) \geq \eta_{\mathrm{SE}}^{\max}$
        $\mathbf{z}^* \leftarrow \mathbf{z}$, $\boldsymbol{\tau}^* \leftarrow \boldsymbol{\tau}$, $\eta_{\mathrm{SE}}^{\max} \leftarrow \tilde{\eta}_{\mathrm{SE}}(\mathbf{z}, \boldsymbol{\tau})$
      **end if**
      **Compute** $o_i$, $\kappa_i$, and $\nu_i$ using (5) and (6) $\forall i$
      **if** KKT conditions are satisfied
        $\mathbf{z}^* \leftarrow \mathbf{z}$, $\boldsymbol{\tau}^* \leftarrow \boldsymbol{\tau}$, **Terminate.**
      **end if**
      $j \leftarrow j - 1$
    **end while**
  **end if**
**end for**

**Algorithm III**

**Input** $\tau_{\min}$, $\tau_{\max,i}$, $\forall i \in \{1, \ldots, K\}$
**Initialize** $j = l = K$, $n = 1$, where $n \equiv |\boldsymbol{\tau}'|$
**for** $l = K : -1 : 1$
  $t \leftarrow \sum_{i=1}^{l-1} \tau_{\max,i} + (K-l)\,\tau_{\min}$
  **if** $t < 1$ and $\tau_{\min} < 1 - t < \tau_{\max,l}$
    $\tau_i \leftarrow \tau_{\max,i}$, $\forall i \leq l-1$ and $\tau_i \leftarrow \tau_{\min}$, $\forall i \geq l+1$
    $\tau_l \leftarrow 1 - t$, $z_i \leftarrow P_{\mathrm{M}}/K$
  **end if**
**end for**

TABLE II
DEFAULT SIMULATION PARAMETERS.

| | | |
|---|---|---|
| $N_0 = 10^{-21}$ W/Hz | $B_{\mathrm{v}} = 20$ MHz | H=6.75 m |
| $P_M = 1000$W | $K = 20$ | $R_{\mathrm{th}} = 50000$ bps |
| $A_{\mathrm{PD}} = 1\,\mathrm{cm}^2$ | $R_{\mathrm{PD}} = 0.6$A/W | $I_o = 1.5 \times 10^{-12}$A |
| $P_{\mathrm{cr}} = 200$ mW | $\tau_{\min} = 7.14 \times 10^{-4}$ | |
| $\psi_{\mathrm{A}} = 85°$ | $\phi_{\mathrm{A}} = 60°$ | |

$(1 - K\tau_{\min})$ is distributed iteratively such that users are allocated their time portions in descending order of channel gains, where in the $i$-th iteration, user $i$ is allocated the minimum between the remaining time budget and the maximum time portion $\tau_{\max,i}$. Then, power is allocated uniformly among users. This way, the complexity of Algorithm III is $O(K)$.

In the next section, we present a comparison between the three algorithms to observe the effect of reducing the computational complexity on the achieved SE performance.

## V. SIMULATION RESULTS

The simulation setup considered consists of a VLC transmitter having 7.6 m clearance form ground, the normal to the transmitter surface is normal to the ground as well. The transmitter coverage is represented by a circle with radius of 38 m, within which we assume $K$ users are uniformly distributed. All the users' receivers are assumed to have horizontal orientation as the transmitter. The average SE results are calculated from 1000 realizations of users placed at random locations according to uniform distribution on the coverage circle surface. The simulation parameters given in Table II are used. In this section, we study of the effect of changing some system parameters on the SE of Algorithm I and compare its performance with Algorithms II, III, and the interior point method algorithm (which is optimal for the considered problem due to its convexity). In the presented simulations, infeasible instances of the optimization problem are considered to have zero SE.

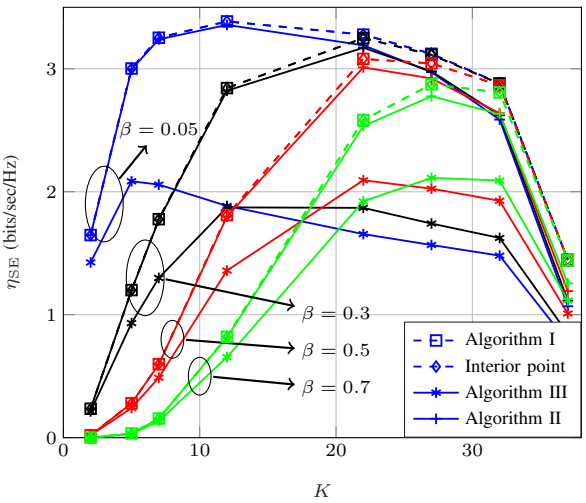


Fig. 2. Average SE vs. number of users, $R_{\mathrm{th}} = 5 \times 10^4$ bps, $P_{\mathrm{M}} = 1$KWatts.

In the first simulation scenario, it can be noticed from Fig. 2 that as the number of users increases, the average SE performance of the system experiences a unimodal behavior; the average SE performance improves till it reaches a peak then it deteriorates till it reaches zero. The average SE increase observed owes to the fact that, as the number of users increases, the probability of having more users experiencing good channels increases which has two direct consequences; it reduces the probability of having infeasible resource allocation problem from an energy harvesting constraint perspective, and gives the transmitter higher degrees of freedom in resource allocation for the feasible instances of the SE optimization problem. On the other hand, the average SE deteriorates beyond some value of $K$ because the resource allocation problem becomes more vulnerable to infeasibility from users worst-case rate perspective; as the number of users increases the worst channel gain experienced by all users gets lower and consequently, minimum required average current to be allocated to each user gets larger, increasing infeasibility. It can be noticed from Fig. 2 that the performance gap between Algorithm I and the other lower complexity algorithms exhibits a unimodal behavior, due to high probability of problem

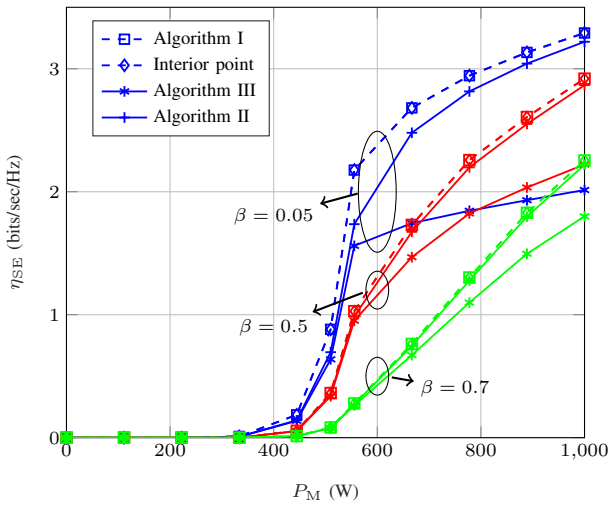


Fig. 3. Average SE vs. total power budget, $R_{\mathrm{th}} = 5 \times 10^4$ bps, $K = 20$.

infeasibility for small and large number of users for the aforementioned reasons.

In the second simulation scenario, the simulation results shown in Fig. 3 show a monotonically increasing SE with the available power budget where at low values for $P_{\mathrm{M}}$ all the problem instances are infeasible. As $P_{\mathrm{M}}$ increases, more realizations of the optimization problem become feasible, and for the feasible instances the feasibility region gets larger, and hence, SE improves. Also, it can be observed that the gap between the optimal performance and Algorithm II performance exhibits a unimodal behavior as $P_{\mathrm{M}}$ increases. because of large proportion of infeasible problems for small $P_{\mathrm{M}}$ values, and the fact that power allocation becomes more significant for large values of $P_{\mathrm{M}}$, which makes Algorithm I lose partially the significance of its superiority over Algorithm II in time allocation. The performance gap between Alogrithm I and Aglorithm III always increases, because Algorithm III uses equal power allocation.

In both simulations, it was found that as the energy harvesting requirement gets tighter, the average SE degrades, and the performance gaps between the three algorithms diminish, because this makes the feasibility region shrink and results in an increasing number of infeasible cases with zero SE. Furthermore, the two simulations have shown that our proposed algorithm achieves a performance that coincides with the interior point algorithm, which is optimal for this problem. In addition, the simulations showed that there is a significant gain from optimization over using Algorithm I.

## VI. Conclusion

We have considered the joint time and power allocation problem for VLC system employing dynamic TDMA. We proposed a KKT-based algorithm to maximize the SE of this setup subject to illumination, power, minimum individual user rate constraint, and energy harvesting constraints. Also, we compared the performance of the proposed algorithm with the optimal solution and suggested two lower complexity algorithms and monitored the effect of reducing complexity on losses in SE performance of the system. The conducted simulations have shown significant gains for our proposed approach, whose performance matched the optimal solution, over the lowest-complexity algorithm.

## VII. Appendix

In this appendix we prove the positive monotonicity of $f(\tau; z, \gamma) = \tau \ln\left(1 + \gamma \frac{z}{\tau}\right)$ with respect to $\tau$ for $0 \leq \tau \leq 1$:

Let us define $g(\tau; z, \gamma)$ as $\frac{\partial f}{\partial \tau} = \ln\left(1 + \frac{\gamma z}{\tau}\right) - \frac{\gamma z/\tau}{1+\gamma z/\tau}$. By calculating the first derivative of $g(\tau; z, \gamma)$ with respect to $\tau$ we get,

$$\frac{\partial g}{\partial \tau} = -\frac{z^2\gamma^2}{\tau^3\left(1 + \gamma z/\tau\right)^2} \leq 0 \tag{16}$$

Since, $g(\tau; z, \gamma)$ is monotonically decreasing in $\tau$ in the interval $0 \leq \tau \leq 1$. Therefore, $\frac{\partial f}{\partial \tau} = \ln\left(1 + \frac{\gamma z}{\tau}\right) - \frac{\gamma z/\tau}{1+\gamma z/\tau} \geq \ln(1 + \gamma z) - \frac{\gamma z}{1+\gamma z}$.

Now, let us consider the function $P(x) = \ln(1+x) - \frac{x}{1+x} = \ln(1+x) + \frac{1}{x+1} - 1$, where $x \in [0, \infty)$ This satisfies $P(0) = 0$, $\lim_{x\to\infty} P(x) = \infty$, $P'(x^*) = \frac{x^*}{(x^*+1)^2} = 0 \Rightarrow x^* = 0$ and $P''(x^*) = \frac{1-x^*}{(x^*+1)^3} \Rightarrow P''(0) = 1 > 0$, which certifies that $x = 0$ is a local minimum for $P(x)$.

Consequently, the global minimum of $P(x)$ for $x \in [0, \infty)$ is zero. Thus, $\ln(1 + \gamma z) - \frac{\gamma z}{1+\gamma z} \geq 0$, which implies that $g(\tau; z, \gamma) \geq 0$ for $0 \leq \tau \leq 1$, which proves the positive monotonicity of $f(\tau; z, \gamma)$ for $0 \leq \tau \leq 1$ and $z \geq 0$.

## References


[1] M. A. Khalighi and M. Uysal, "Survey on free space optical communication: A communication theory perspective," *IEEE Commun. Surveys Tuts.*, vol. 16, no. 4, pp. 2231–2258, Jun. 2014.

[2] P. H. Pathak, X. Feng, P. Hu, and P. Mohapatra, "Visible light communication, networking, and sensing: A survey, potential and challenges," *IEEE Commun. Surveys Tuts.*, vol. 17, no. 4, pp. 2047–2077, 2015.

[3] A. M. Abdelhady, O. Amin, A. Chaaban, and M.-S. Alouini, "Downlink resource allocation for multichannel tdma visible light communications," in *Proc. IEEE Global Conf. Signal and Inform. Process. (GlobalSIP)*, Washington DC, 2016, pp. 1–5.

[4] M. Uysal, Z. Ghassemlooy, A. Bekkali, A. Kadri, and H. Menouar, "Visible light communication for vehicular networking: performance study of a v2v system using a measured headlamp beam pattern model," *IEEE Veh. Technol. Mag.*, vol. 10, no. 4, pp. 45–53, Dec. 2015.

[5] I. Takai, T. Harada, M. Andoh, K. Yasutomi, K. Kagawa, and S. Kawahito, "Optical vehicle-to-vehicle communication system using led transmitter and camera receiver," *IEEE Photon. J.*, vol. 6, no. 5, pp. 1–14, Oct. 2014.

[6] J. M. Kahn and J. R. Barry, "Wireless infrared communications," *Proceedings of the IEEE*, vol. 85, no. 2, pp. 265–298, Feb 1997.

[7] A. Lapidoth, S. M. Moser, and M. Wigger, "On the capacity of free-space optical intensity channels," *IEEE Trans. Inf. Theory*, vol. 55, no. 10, pp. 4449–4461, Oct. 2009.

[8] T. Rakia, H. C. Yang, F. Gebali, and M. S. Alouini, "Optimal design of dual-hop vlc/rf communication system with energy harvesting," *IEEE Commun. Lett.*, vol. 20, no. 10, pp. 1979–1982, Oct 2016.

[9] S. Boyd and L. Vandenberghe, *Convex optimization*. Cambridge university press, 2004.

[10] R. M. Corless, G. H. Gonnet, D. E. Hare, D. J. Jeffrey, and D. E. Knuth, "On the lambertw function," *Advances in Comput. Math.*, vol. 5, no. 1, pp. 329–359, 1996.